Targeted energy pumping using a linear complex attachment

N. Roveri[1], A. Carcaterra[1,3], A. Akay[2,3]
[1]Department of Mechanics and Aeronautics, University of Rome, "La Sapienza"
Via Eudossiana, 18, 00184, Rome, Italy
email: **nicola.roveri@uniroma1.it**

[2]Department of Mechanical Engineering, Bilkent University
Ankara, Turkey 06800

[3]Department of Mechanical Engineering, Carnegie Mellon University
Pittsburgh, Pennsylvania 15213

Abstract
The present paper considers the problem of realizing an effective targeted energy pumping from a linear oscillator to a plurality of ungrounded linear resonators, attached to it in parallel. Theoretical as well as numerical results demonstrate the efficacy of using a complex attachment as a passive absorber of broadband energy, injected into the primary structure. The paper unveils also the existence of an instantaneous frequency associated to the master response characterized by intermittency: a rather surprising result for a linear autonomous system. A comparative analysis with a nonlinear energy sink demonstrates that the two systems present some analogies in this respect and that the complex attachment is a very efficient energy trap.

1 Introduction

In the past three decades a number of new devices have been invented and employed for the absorption of stationary and transient vibrations of many types of engineering structures [1-14]. Conventional devices designed for civil structures are generally linear and require the addition of large masses to the primary structure, which makes these systems of limited interest. Moreover, they are effective over a narrow frequency range, showing poor performance in case of broadband inputs, such as earthquakes. To overcome these problems, nonlinear techniques for vibration absorption have been extensively studied [1-6]. One such method involves the use of a weakly nonlinear vibration absorber, added to the principal structure, that can operate under various types of external excitation [1]. Damping in the absorber plays a fundamental role and governs the effective bandwidth of absorption: thus a tradeoff exists between attenuation efficiency and bandwidth, which narrows the range of applicability. Strongly nonlinear passive absorbers have also been investigated [2-5], that generally provide better performance than the corresponding linear and weakly nonlinear devices, leading to a targeted energy pumping into the nonlinear absorber. Energy pumping corresponds to a controlled and irreversible transfer of the vibrational energy, from the main structure, to a passive, essentially nonlinear, attachment, where it remains trapped and eventually dissipated; the attachment acts as a nonlinear energy sink (NES). A number of papers have shown that a proper design of the absorbing structure permits a nonlinear mode of vibration, which leads to energy pumping [3]. Unlike common linear and weakly nonlinear devices, strong nonlinear attachments are effective over a rather wide range of frequencies [4]. Despite the important advantages of using NES, they are accompanied by some drawbacks. One is the existence of extra branches of periodic regimes: under certain conditions relevant vibrations may be induced by the NES, much higher than those of the linear system, and thus may be catastrophic. Another drawback is that energy pumping activates only

above a specific energy value: when the vibratory energy is below a threshold level, NES is not effective [5]. Finally, a small mass for the NES is required for an efficient application to real structures [5].

Research on nonlinear attachments has been focused on finding methods for efficient energy pumping. It is well known that irreversibility, in physical systems with a finite number of degrees of freedom, develops as a consequence of nonlinearities [6]. Nonlinearity destroys the periodic motion in linear systems [7], and as a consequence the energy remains widely spread among the degrees of freedom, and never reorganizes itself to return to its source, giving rise to irreversibility. However, weak nonlinearities are not as effective in producing irreversibility: this result has been empirically confirmed [1], and holds in general for Hamiltonian isochronous or non-isochronous systems, as stated by the Nekhoroshev's theorem [8], or by the complementary and more celebrated Kolmogorov–Arnold–Moser theorem, respectively. In a nutshell, the theorems show the motion of a weakly nonlinear system remains very close to that of the corresponding linearized system, without developing irreversibility.

These arguments suggest that irreversibility (i) is a result of strong nonlinearities and (ii) does not take place in linear systems, because their modal energies are constants of motion. However, this notion requires deeper investigations in the light of results from a special class of linear systems [9-14], which exhibits an irreversible energy transfer. These systems consist of a principal structure, called master, which is a one dimensional resonator, coupled to a large number of parallel resonators, constituting the attachment. The whole system is linear but its special architecture allows a very effective energy pumping, from the principal to the attachment, which acts as a linear energy sink (LES). We refer to the whole system simply as master-attachment, while complex attachment (CoAt) is adopted for the satellite structure.

In spite of the rich literature on the subject, there still exists a number of issues related to the use of a CoAt for targeted energy transfer, that deserve to be further investigated. The attention in the early studies has been mainly focused on the early stage of the energy sharing process, after that the motion of the master undergoes a transition, from an almost-periodic to a random like motion, a process that has not completely understood. Other important issues that arise from these arguments include whether apparent damping is actually an irreversible phenomenon and if LESs may be better suited than NESs for efficient energy pumping. The purpose of this paper is to provide theoretical and numerical insights into these open questions. The structure of the paper is as follows: in section 2 the basic phenomenology of a CoAt is presented, a comparative study with an essentially nonlinear attachment is also provided. In section 3 a theoretical model describing the mechanism behind apparent damping is discussed, the model is validated with numerical experiments, using the empirical mode decomposition and the normalized Hilbert transform [15]. Section 4 contains concluding remarks.

2 Energy sinks: comparison linear versus nonlinear

The prototype linear system representing a one-dimensional oscillator coupled to a set of parallel oscillators is depicted in Fig.1.

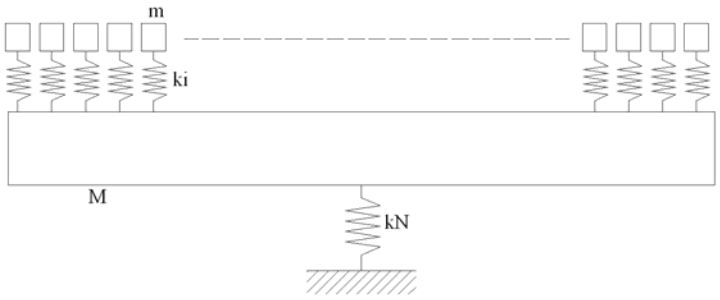

Figure 1: Prototype of master-attachment system.

The complex attachment is characterized by a large number of resonators, typically more than 100; the word complex is used to underscore the large number of resonators within the satellite. The special architecture of the attachment plays a fundamental role in producing an effective energy pumping, and allows a total mass which is a small fraction that the master, typically 1/10. A short description of the observed phenomena is given ahead.

As the primary structure is excited, the injected energy E_{tot} flows quickly to the CoAt: nearly the whole energy remains stored in it up to the time t^* [9,11], called the return time. At t^* most of the energy reorganizes to return to the master. This phenomenon is called apparent damping because, although none energy dissipation is involved in this conservative system, the master reacts as a damped resonator up to t^*. Typical time history of the master displacement is shown in Fig. 2.

Observing the phenomena in the long time range ($t^*<t<30t^*$), different energy sharing processes are displayed as in Fig. 3: (i) at early stage the energy is periodically transferred to and from the primary, (ii) the energy peaks become progressively less energetic and (iii) the periodicity of the energy transfers is progressively lost, (iv) the motion of the master approaches a random noise about a mean value and (v) nearly the whole energy remains trapped within the CoAt.

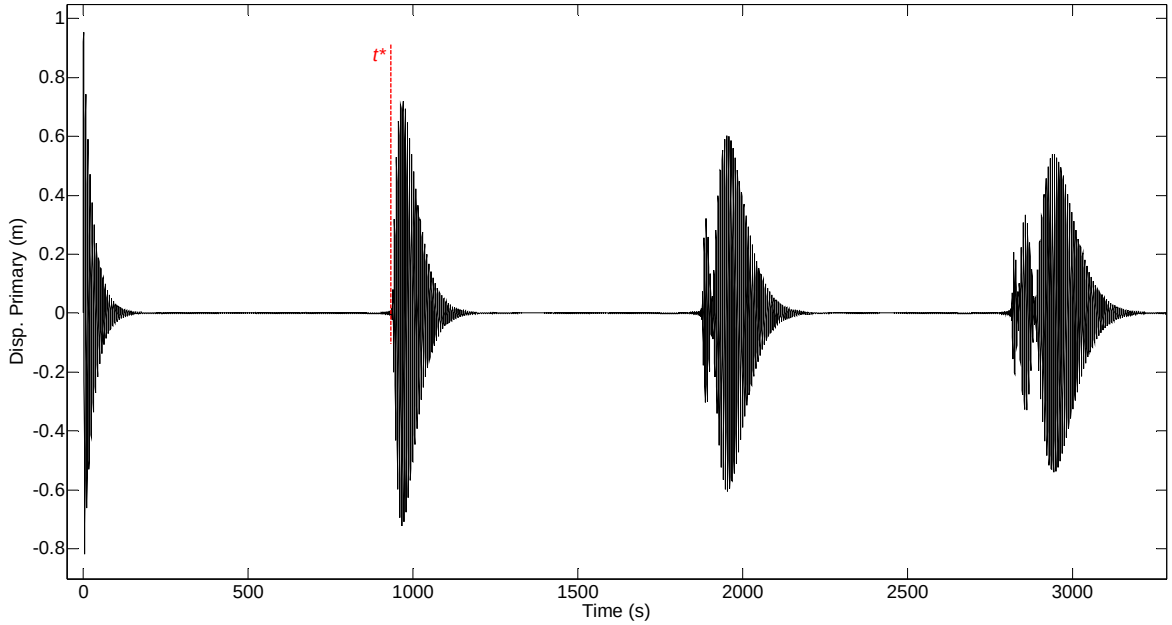

Figure 2: Example of apparent damping for an impulsive excitation of the master, E_{tot} is 0.5 *J*.

When a small amount of dissipation is included, differences among motions of conservative and dissipative master-attachment systems become appreciable only in long times: the energy of the damped system tends in this case to zero.

The free vibrations of a master-attachment system with N degrees of freedom are described by the equations:

$$\begin{cases} m\ddot{x}_j(t) + k_j\left(x_j(t) - x_N(t)\right) = 0 \qquad j = 1,2..N\text{-}1 \\ M\ddot{x}_N(t) + k_N x_N(t) + \sum_{j=1}^{N-1} k_j\left(x_N(t) - x_j(t)\right) = 0 \end{cases} \tag{1}$$

where the index N is for the master and 1, 2,.., N-1 for the oscillators of the attachment; m is the uniform mass of each oscillator of the attachment, k_j, M, k_N, $x_j(t)$ and t are the stiffness of each oscillator of the attachment, the mass and the stiffness of the master, the displacement of the *j-th* oscillator and time, respectively.

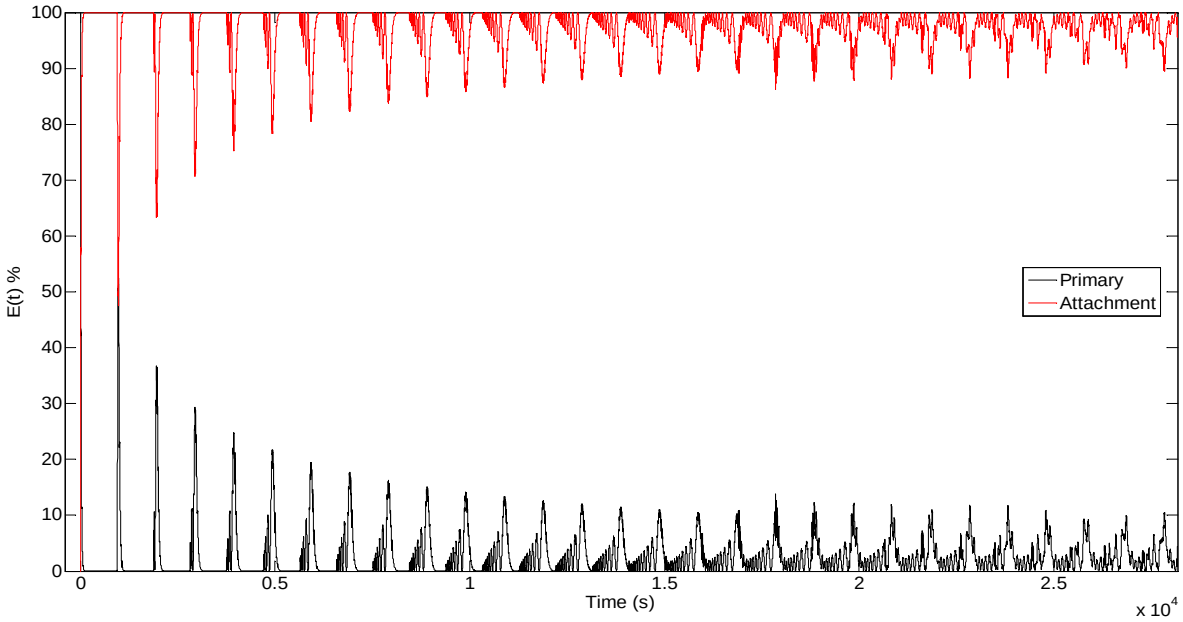

Figure 3: Percentage of the instantaneous time energy within the master and the CoAt, respectively, where $E_{attach}(t)=(1-E_N(t)/E_{tot})$, plotted versus time, for a linear frequency distribution.

The apparent damping effect develops only when the master frequency $\omega_M = \sqrt{k_N/M}$ belongs to the frequency interval $B = [\omega_{01}, \omega_{0N-1}]$ described by the uncoupled frequencies of the oscillators within the attachment, i.e. $\omega_{0i} = \sqrt{k_i/m}$.

Considering eq. (1), the use of modal coordinates $\boldsymbol{\eta}$ through the eigenvector matrix $\mathbf{U}$ produces $\mathbf{x} = \mathbf{U}\boldsymbol{\eta}$, and choosing as initial conditions an impulse of velocity V_0 acting on the master, i.e. $\mathbf{x}(0) = \mathbf{0}$, $\dot{\mathbf{x}}(0) = (0, \cdots, 0, V_0)^T$, through the use of modal analysis, the displacement and the velocity of each resonator are:

$$x_i(t) = \sum_{j=1}^{N} \omega_j^{-1} U_{ij} \sqrt{2E_j}\, sin(\omega_j t), \quad \dot{x}_i(t) = \sum_{j=1}^{N} U_{ij} \sqrt{2E_j}\, cos(\omega_j t) \tag{2}$$

where ω_j's and E_j's are the eigenvalues and the modal energies of the system, respectively, namely the energies of the modal resonators:

$$E_j = ME_{tot}U_{Nj}^2$$

with $E_{tot} = MV_0^2/2$. From eq. (2), the displacement of the primary structure is rewritten as follows:

$$x_N(t) = \sum_{j=1}^{N} a_j\, sin(\omega_j t) \tag{3}$$

where $a_j = V_0 E_j / (\omega_j E_{tot})$.

As a fundamental parameter in monitoring the energy sharing process, the energy of the master is defined:

$$E_N(t) = 0.5M\left(\dot{x}_N^2(t) + \omega_M^2 x_N^2(t)\right) \tag{4}$$

The energy ratios $E_N(t)/E_{tot}$ and $E_{attach}(t)=\left(1-E_N(t)/E_{tot}\right)$ are used as indicators of the energy spreading among the resonators, they are shown in Fig. 3.

Substituting eq. (3) into eq. (4), the energy of the master becomes:

$$E_N(t)=\sum_{j=1}^{N}\sum_{q=1}^{N}\frac{E_jE_q}{E_{tot}}\left(cos\,\varphi_j(t)cos\,\varphi_q(t)+\frac{\omega_M^2}{\omega_j\omega_q}sin\,\varphi_j(t)sin\,\varphi_q(t)\right) \tag{5}$$

where $\varphi_j(t)=\omega_j t$ is the phase-angle. Under the hypothesis of B small enough $\omega_M^2/\omega_j\omega_q\approx 1,\ \forall j,q$, thus the nondimensional energy becomes:

$$\varepsilon(t)\approx[\varepsilon_N]+\sum_{j\neq q}\varepsilon_j\varepsilon_q cos\left(\omega_j-\omega_q\right)t \tag{6}$$

where $\varepsilon_j=E_j/E_{tot}$ is the normalized modal energy. It is possible to show [13] that:

$$[\varepsilon_N]=\lim_{t\to\infty}\frac{1}{T}\int_0^T\frac{E_N(t)}{E_{tot}}dt\approx\frac{1}{N} \tag{7}$$

As shown in Fig. 3, the energy peaks are progressively less energetic and, after an initial transient, they remain close to the mean value (7), which can be made negligibly small by simply increasing the number of resonators. The complexity of the satellite plays a fundamental role in producing effective energy storage within the attachment: through a proper selection of N it is possible to select the residual energy that remains with the master.

Fig. 3 also shows the energy fluxes between the primary and the CoAt, equipped with equispaced frequencies, i.e. $\omega_{0i}=i2\omega_M/(N-1)$ within the bandwidth $B=\left[\omega_M/(N-1),2\omega_M\right]$, which we refer as linear distribution. For an impulsive excitation of the master, where $\dot{x}_N(0)=1$ *m/s*, and with the following parameters N=300, M=1 *kg*, $\varepsilon=m(N-1)/M=0.1$, $\omega_M=1$ *rad/*. It appears more than 85% of the energy remains stored within the satellite structure.

To check the effectiveness of the CoAt, the results are compared with that of a linear oscillator coupled to a NES [5]. The system consists of a linear oscillator, of mass m_1 and stiffness k_1, coupled through an essentially nonlinear stiffness k_2 to a mass m_2, the equations of motion are:

$$\begin{cases}\ddot{x}_1+\omega_1^2x_1+\lambda_1\dot{x}_1+\lambda_2\left(\dot{x}_1-\dot{x}_2\right)+\omega_2^2\left(x_1-x_2\right)^3=0\\ \varepsilon\ddot{x}_2-\lambda_2\left(\dot{x}_1-\dot{x}_2\right)-\omega_2^2\left(x_1-x_2\right)^3=0\end{cases} \tag{8}$$

where $\omega_1=\sqrt{k_1/m_1}$, $\omega_2=\sqrt{k_2/m_1}$, $\varepsilon=m_2/m_1$, $\lambda_1=c_1/m_1$, $\lambda_2=c_2/m_1$, with c_1 and c_2 the damping coefficient. As a first example, Fig. 4 shows the exchanges of energy after the impulsive excitation of the undamped linear oscillator, with the following parameters: $\dot{x}_1(0)=1$ *m/s*, $\varepsilon=0.1$, $\omega_1=\omega_2=1\ rad/s$.

Even if a nonlinear spring is interposed between the primary and the attachment, the energy is periodically transferred back and forth from the linear oscillator, namely the energy transfer is not irreversible, unlike the case for Fig. 3. This result is not surprising, since Lee *et al* [5] demonstrated that a nonlinear beat phenomenon takes place between the linear oscillator and the NES. As a second example, the same system is studied in this case with light damping, $\lambda_1=\lambda_2=0.0015$. Again, Fig. 5 shows how the undamped response of the master decays much faster than the one of the damped linear oscillator with the NES.

These simple but significant examples demonstrate the capability of CoAt to trap the vibratory energy much more effectively than a corresponding NES. This conclusion will be corroborated with theoretical and numerical results in the forthcoming section.

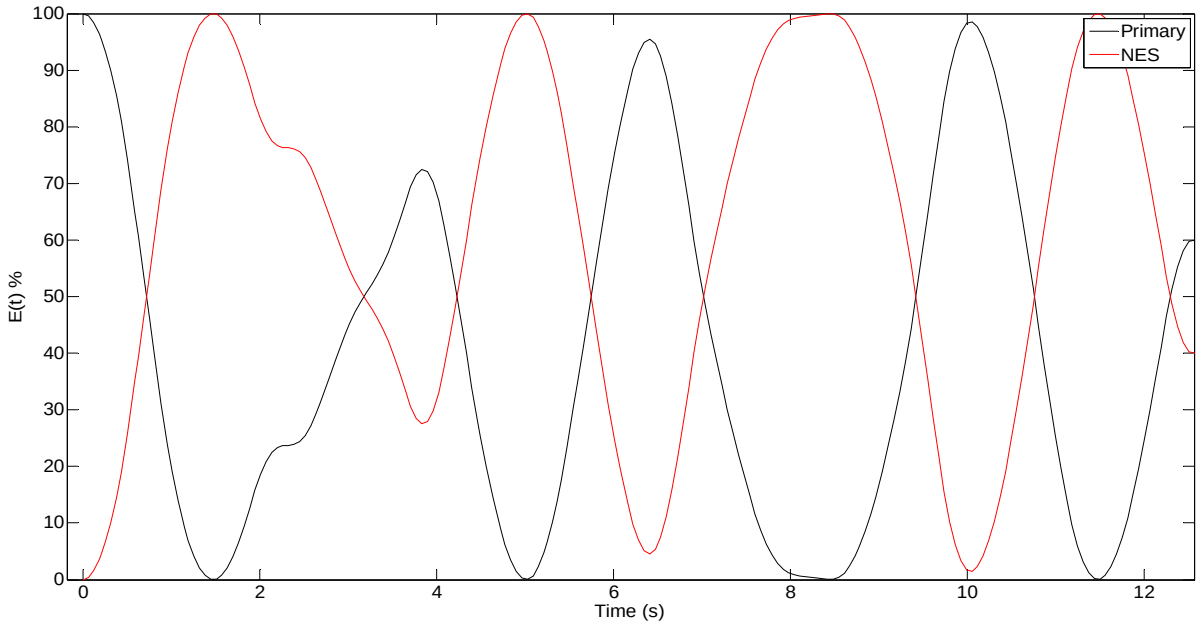

Figure 4: Percentage of the instantaneous energy in the linear oscillator and the NES, respectively.

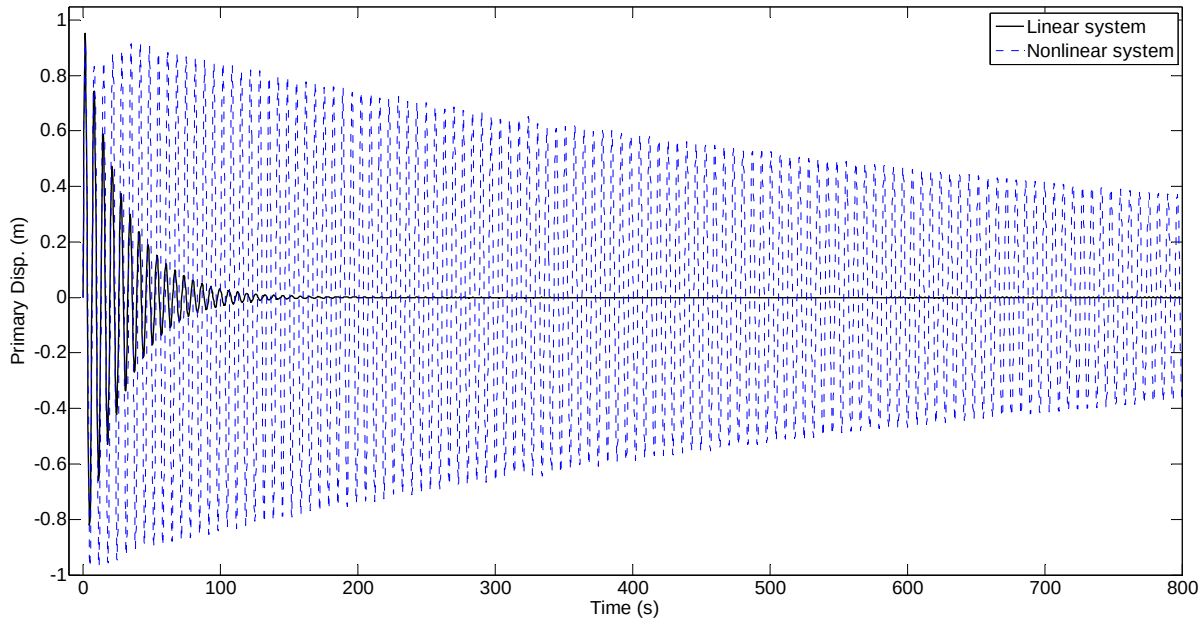

Figure 5: Displacement of primary structures coupled to a LES and to a NES, respectively.

3 Energy pumping in linear systems with a complex attachment

3.1 Master response decomposition

Equation (7) only provides information regarding the average motion and does not prevent localized (in time) energy returns to the master, which are caused by constructive interference among the modal components in eq.s (3) and (6). Thus, to get insight into the energy sharing process, it is important to study the way the modal components interact over time.

For a system equipped with a linear frequency distribution within the attachment, the spectrum of the coefficients a_j and of the modal energies E_j are nearly symmetric with respect to the vertical axis passing through the mode index j_0, slightly smaller than $N/2$, as depicted in Fig. 6 for N=300 and $j_0 = 144$.

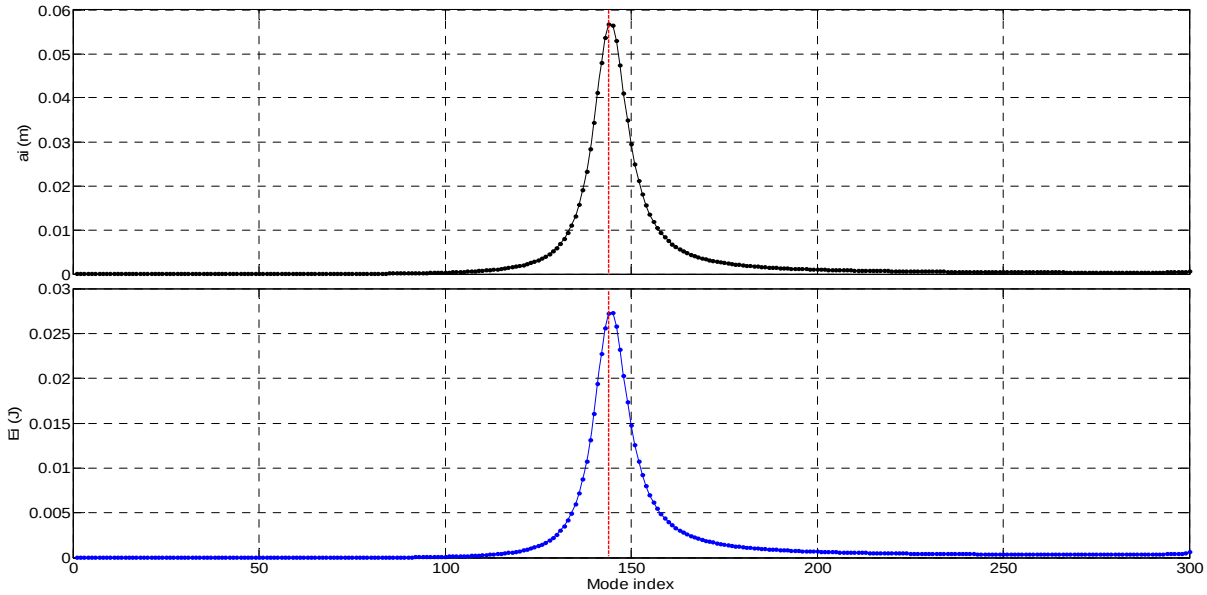

Figure 6: Starting from the subplot on top, amplitude and modal energy spectra, respectively, plotted versus the mode index j, the symmetry axis is depicted in dashed line.

Then:

$$a_{j_0+j} \approx a_{j_0-j+1},\ j = 1,2,..j_0 \tag{9}$$

and eq. (3) is rearranged as follows:

$$x_N(t) = \left[\sum_{j^-=1}^{j_0} a_{j^-}\, sin\left(\omega_{j^-} t\right) + \sum_{j^+=j_0+1}^{2j_0} a_{j^+}\, sin\left(\omega_{j^+} t\right)\right] + \sum_{j=2j_0+1}^{N} a_j\, sin\left(\omega_j t\right)$$

using eq. (9), the previous equation can be approximated as:

$$x_N(t) \approx \left[\sum_{j^-=1}^{j_0} a_{j^-}\left(sin\left(\omega_{j^-} t\right) + sin\left(\omega_{j^+} t\right)\right)\right] + \sum_{j=2j_0+1}^{N} a_j\, sin\left(\omega_j t\right)$$

then, the prosthaphaeresis formulas lead to:

$$x_N(t) \approx \left[\sum_{j=1}^{j_0} 2c_j\, cos\left(\frac{\omega_{j^+} - \omega_{j^-}}{2} t\right) sin\left(\frac{\omega_{j^+} + \omega_{j^-}}{2} t\right)\right] + \sum_{j=2j_0+1}^{N} a_j\, sin\left(\omega_j t\right)$$

where $c_j = a_{j_0-j+1}$, $j^- = j_0 - j + 1,\ j^- \in [1, j_0]$ and $j^+ = j_0 + j,\ j^+ \in [j_0+1, 2j_0]$, respectively. Considering $\left(\omega_{j^+} + \omega_{j^-}\right)/2 \approx \omega_M$ and $\sum_{j=2j_0+1}^{N} a_j\, sin\left(\omega_j t\right) \approx a_{HF}\, sin\left(\omega_{HF} t\right)$, with $a_{HF} = \sum_{j=2j_0+1}^{N} a_j$ and $\omega_{HF} = \sum_{j=2j_0+1}^{N} \omega_j / \left(N - 2j_0\right) \approx 2\omega_M$, and setting $\Delta\omega_j = \left(\omega_{j^+} - \omega_{j^-}\right)/2$, eq. (3) is approximated as the sum of two terms:

$$x_N(t) \approx x_{beat}(t) + x_{HF}(t) \tag{10}$$

where:

- $x_{beat}(t) = \sum_{j=1}^{j_0} 2c_j \cos(\Delta\omega_j t) \sin(\omega_M t)$ is the sum of the beat components, that have the same carrier wave $\sin(\omega_M t)$ while modulated by different envelopes $2c_j \cos(\Delta\omega_j t)$;
- $x_{HF}(t) = a_{HF} \sin(2\omega_M t)$ is a low energy high-frequency wave that vibrates at twice the master frequency.

Hilbert transform of eq. (10) allows evaluation of the analytic signal and the instantaneous amplitude and phase, yielding:

$$\hat{x}_N(t) = \mathrm{H}(t)\left(A(t)e^{i\omega_M t} + a_{HF}e^{i2\omega_M t}\right) \tag{11}$$

where the modulation theorem [16] has been used, $\mathrm{H}(t)$ is the Heaviside step function, *i* the imaginary unit, and:

$$A(t) = \sum_{j=1}^{j_0} 2c_j \cos(\Delta\omega_j t) \tag{12}$$

is the envelope of $x_{beat}(t)$. Expressing eq. (11) in polar form:

$$\hat{x}_N(t) = X(t)e^{i\varphi(t)t} \tag{13}$$

where:

$$X(t) = \mathrm{H}(t)\sqrt{A^2(t) + a_{HF}^2 + 2A(t)a_{HF}\cos(\omega_M t)},\ \varphi(t) = \frac{A(t)\sin(\omega_M t) + a_{HF}\sin(2\omega_M t)}{A(t)\cos(\omega_M t) + a_{HF}\cos(2\omega_M t)} \tag{14}$$

together form the canonical pair associated with $\hat{x}_N(t)$. The instantaneous frequency is defined as the time derivative of the phase function $\varphi(t)$:

$$\omega(t) = X^{-2}(t)\left(A^2(t)\omega_M + a_{HF}^2 2\omega_M - a_{HF}\dot{A}(t)\sin(\omega_M t) + 3A(t)a_{HF}\omega_M\cos(\omega_M t)\right) \tag{15}$$

where $\dot{A}(t)$ is $dA(t)/dt$. Eq.s (10, 11, 14, 15) suggest that:

i. as the interference between the beats is constructive $A(t) \gg a_{HF}$ thus $X(t) \approx \mathrm{H}(t)A(t)$ and $\omega(t) \approx \omega_M$: the frequency of motion of the primary is not influenced by the satellite structure, while its amplitude is controlled by the envelope of $x_{beat}(t)$;

ii. when the interference among the beats is destructive, $A(t) \approx 0$, thus $X(t) \approx \mathrm{H}(t)a_{HF}$ and $\omega(t) \approx 2\omega_M$: the frequency of motion of the master is twice the uncoupled frequency, its vibrations are controlled by the low energy, high-frequency, modal components;

iii. if $A(t)$ undergoes a rapid variation, the term controlled by $\dot{A}(t)$ introduces a frequency modulation around the carrier frequency.

It appears that the envelope of $x_{beat}(t)$ has a fundamental role on the dynamics of the energy pumping. The time evolution of $A(t)$ is indeed analysed in the next section.

3.2 Frequency intermittency effects

It is possible to prove that the eigenfrequencies nearly coincide with the uncoupled frequencies [26], thus for a linear frequency distribution within the attachment, the uncoupled frequencies of the satellite structure are: $\omega_{0i} = i2\omega_M/(N-1)$, $i = 1, 2..N-1$, and the eigenfrequencies are approximated as follows:

$$\omega_s \approx s2\omega_M/N, \quad s = 1, 2..N \tag{16}$$

Using eq. (16) into eq. (12), $\Delta\omega_j$ becomes:

$$\Delta\omega_j = 0.5\left(\omega_{j^+} - \omega_{j^-}\right) \approx (2j-1)\omega_M/N, \quad j = 1, 2..j_0 \tag{17}$$

Eq. (17) has been numerically validated, the frequencies in eq. (12) are roughly odd multiples of the fundamental frequency $\Omega = \Delta\omega_1 \approx \omega_M/N$. Through eq. (17), eq. (12) becomes a summation of harmonic functions:

$$A(t) \approx \sum_{s=1}^{j_0} 2c_s \cos\left(s_{odd}\Omega t\right) \tag{18}$$

with $s_{odd} = 2s-1$. Since $c_s/c_{s-1} \approx \alpha \rightarrow c_s \approx \alpha^{s-1}c_1$, with $\alpha < 1$, and using the Euler's formula eq. (18) is:

$$A(t) \approx \sum_{s=1}^{j_0} c_s\left(e^{i(2s-1)\Omega t} + e^{-i(2s-1)\Omega t}\right)$$

and then:

$$A(t) \approx \frac{c_1}{\alpha}\left[e^{-i\Omega t}\left(\sum_{s=0}^{j_0}\left(\alpha e^{i2\Omega t}\right)^s - 1\right) + e^{i\Omega t}\left(\sum_{s=0}^{j_0}\left(\alpha e^{-i2\Omega t}\right)^s - 1\right)\right] \tag{19}$$

Both summations are geometric series, thus:

$$A(t) \approx \Delta a \cos(\Omega t)/(1-\cos(2\Omega t)) \tag{20}$$

where $\Delta a = a_{j_0} - a_{j_0-1}$ is the amplitude gap between the two most energetic modes. Each summation in eq. (19) reminds of a Dirichlet kernel, which is a periodic, rapidly changing function, and gives eq. (20) the following properties:

- *A(t)* is approximated by a periodic function of period $T_{beat} = \pi/\Omega$;
- the approximated expression of *A(t)* has a sharp decay around the extrema, located at $0, T_{beat}, 2T_{beat}, ..$, and decays as $1/(2\Omega t)^2$.

In light of the previous results, the instantaneous frequency of the primary is expected to display intermittency between ω_M and $2\omega_M$: eq. (20) shows that the beat components have constructive interference in the neighborhood of $0, T_{beat}, 2T_{beat}, ..$, thus $A(t) \gg a_{HF}$ and eq. (15) is dominated by ω_M, outside these neighborhoods, the beat components have destructive interference and $A(t) \approx 0$, and eq. (15) is then controlled by the high frequency component $2\omega_M$. It is worth underlining the frequency jump, from ω_M to $2\omega_M$, of the primary structure, is quite surprising, particularly considering the whole system is linear and autonomous and, to the authors' knowledge, has never been reported before. In fact, for a linear system the attachment does not act as a purely damping effect [11], but indeed produces frequency switching effect as shown. On the other hand, a similar frequency jump is observed in a NES only when a trigger energy value is reached [5].

3.3 Numerical experiments and discussion

To evaluate the accuracy of the aforementioned results, numerical examples are presented. Fig. 7 shows the envelope defined by eq. (12), observations about the accuracy of eq. (20) follow:

- eq. (20) provides qualitative information at the early stage of motion, since *A(t)* has sharp peaks in the neighborhood of $0, T_{beat}, 2T_{beat}, \ldots$, while it approaches zero outside these neighborhoods;
- with increasing time, eq. (20) becomes less accurate, since the extrema of *A(t)* become less sharp, while more and more ripples precede each extremum, as a consequence the time intervals where $A(t) \approx 0$ progressively reduce to zero.

The inadequacy of eq. (20) to estimate *A(t)* for long times is a consequence of the harmonic approximation (17). More precisely, the small errors committed in eq. (17), involving the eigenfrequencies, are negligible at early stage, but progressively destroy the strict periodicity of motion predicted by eq. (20). This suggests, a transition in the nature of motion is taking place: a more accurate model is indeed needed to describe the interaction of the modal components after the early stage of motion.

To verify the existence of an intermittent frequency and more generally, to get insightful information concerning the energy sharing process, the transient response of the master is processed with the empirical mode decomposition (EMD) and the normalized Hilbert transform (NHT) [15]. EMD is a well established method that can be used to decompose a signal in terms of monocomponent functions called intrinsic mode functions (IMFs), which can be thought as intrinsic oscillatory modes imbedded in the data. NHT is an empirical technique designed to separate the AM and FM parts of each IMF, it allows evaluating the instantaneous frequency (IF) of the IMF without the use of the Hilbert transform (HT), since direct application of the HT is often problematic and may produce meaningless results, as pointed out in [15]. After the master response has been processed via EMD, only two IMFs are generated: since the energy of the second IMF is much smaller than the first one (roughly 1/100), only the first IMF is considered. This confirms the assumption made in section 3.1, where the master response was assumed monocomponent.

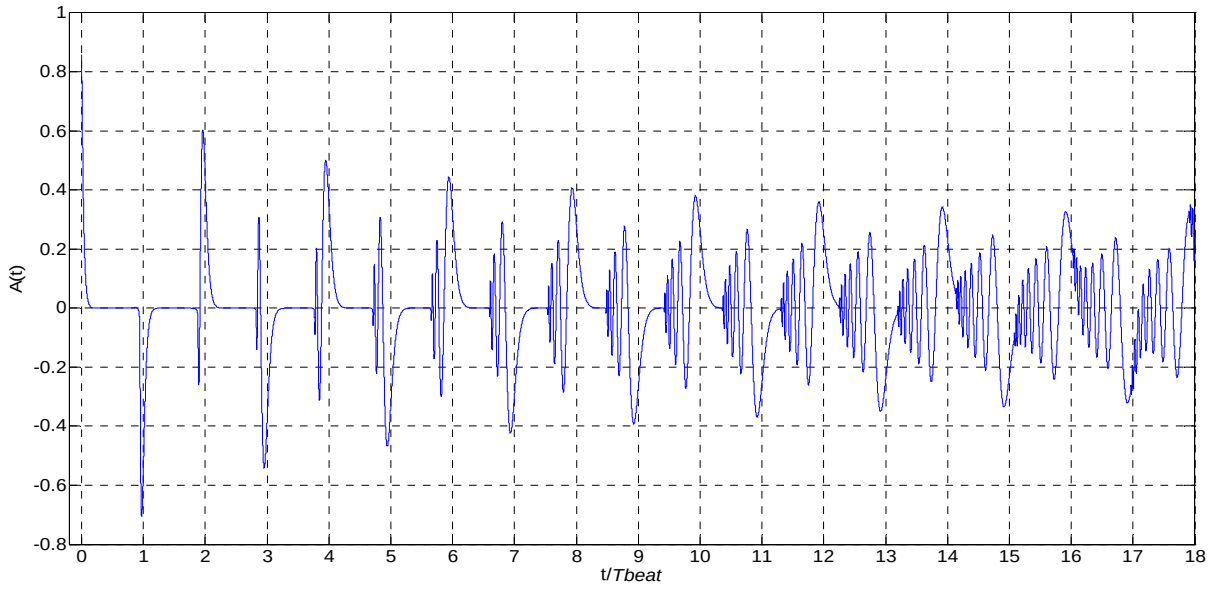

Figure 7: The envelope *A(t)* plotted versus the normalised time t/T_{beat}.

Fig. 8 shows the first IMF, its instantaneous amplitude and frequency, respectively, obtained with NHT. Numerical results are in good agreement with predictions made by eq.s (15, 20):

- there exists an initial transient where the master has a damped response and the envelope has a sharp decay, followed by a stationary state where its value is approximately zero, for $t \approx T_{beat}$ the envelope regains a sharp crest and most of the energy is returned to the master;
- the instantaneous frequency is initially equal to ω_M, due to the rapid variation of the envelope, the term controlled by $\dot{A}(t)$ introduces a frequency modulation and causes higher and higher fluctuations around the carrier frequency ω_M, as described by the sinusoidal term in eq. (15) and as discussed in [15];
- there is a frequency jump from ω_M to $2\omega_M$ as the instantaneous amplitude reaches the trigger value at $t/T_{beat} \approx 0.18$. Fig. 9 shows a close-up of the master response during the time interval $t/T_{beat} = [0.15, 0.3]$: the frequency doubling is clear;
- corresponding to the sharp rise of the envelope, at $t/T_{beat} \approx 0.95$, a backward frequency jump, from $2\omega_M$ to ω_M, takes place.

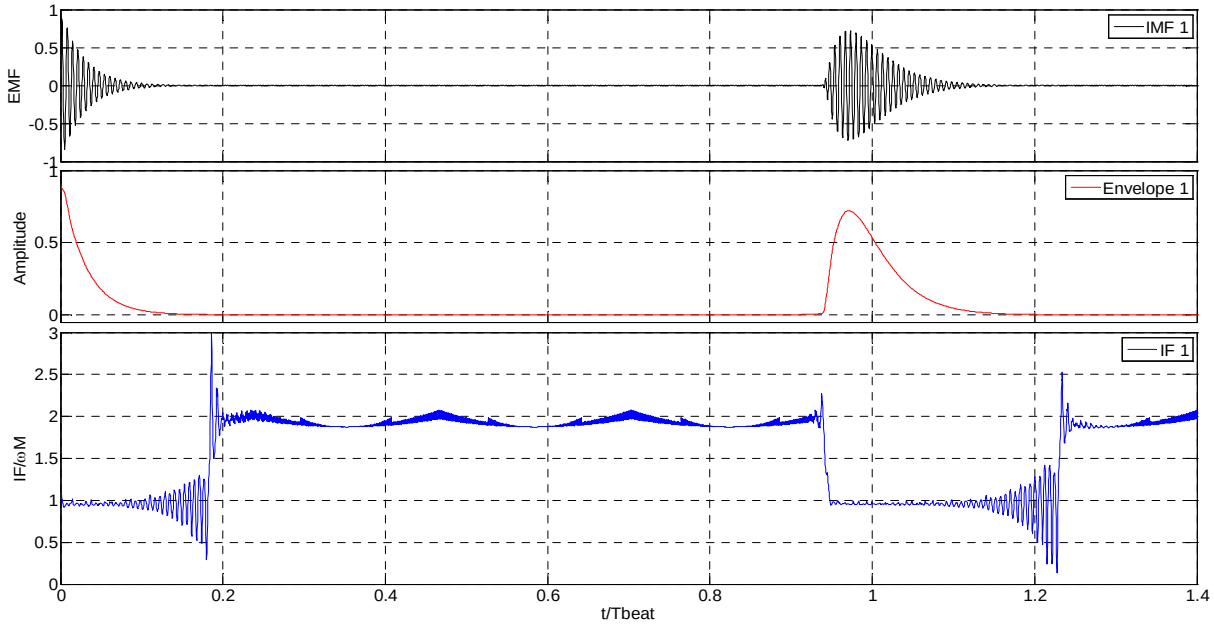

Figure 8: Starting from the subplot on top, the first IMF of the master displacement, the instantaneous amplitude and normalized frequency, plotted versus the normalised time t/T_{beat}.

Fig. 10 shows a frequency-energy plot of $E_N(IF(t))$, within the time interval t/T_{beat}=[0,0.97]; at t/T_{beat}=0.97 the energy returned to the master has a maximum. The graph is in the form of a loop, sketched in dashed line in figure:

- there exists an initial transient where the primary is in resonance with the most energetic resonators, and during this phase the energy is almost monotonically transferred from the master, to the satellite structure: the vibrations of motion have frequency roughly equal to ω_M, and the satellite acts as a damper. It is worth to notice that the numerical IF is slightly smaller than ω_M because, in section 3.1 j_0 is slightly smaller than $N/2$ then $0.5\left(\omega_{j^+} + \omega_{j^-}\right) < \omega_M$;
- as nearly the whole energy is transferred to the satellite, the IF experiences a sudden jump, from ω_M to $2\omega_M$: the primary and the most energetic resonators remain energetically decoupled and, as a consequence, the energy is trapped within the satellite structure. The master is now in resonance with a few, low energy, high-frequency resonators, and exchanges energy with them in a reversible fashion;

- as the master energy reaches the trigger value, roughly 10^{-4} *J*, a backward jump takes place, which brings the IF back to ω_M, during this phase most of the energy is rapidly returned to the master;
- the ending point of the loop does not coincide with the starting point, showing there is a part of the energy which remains irreversibly trapped into the satellite structure.

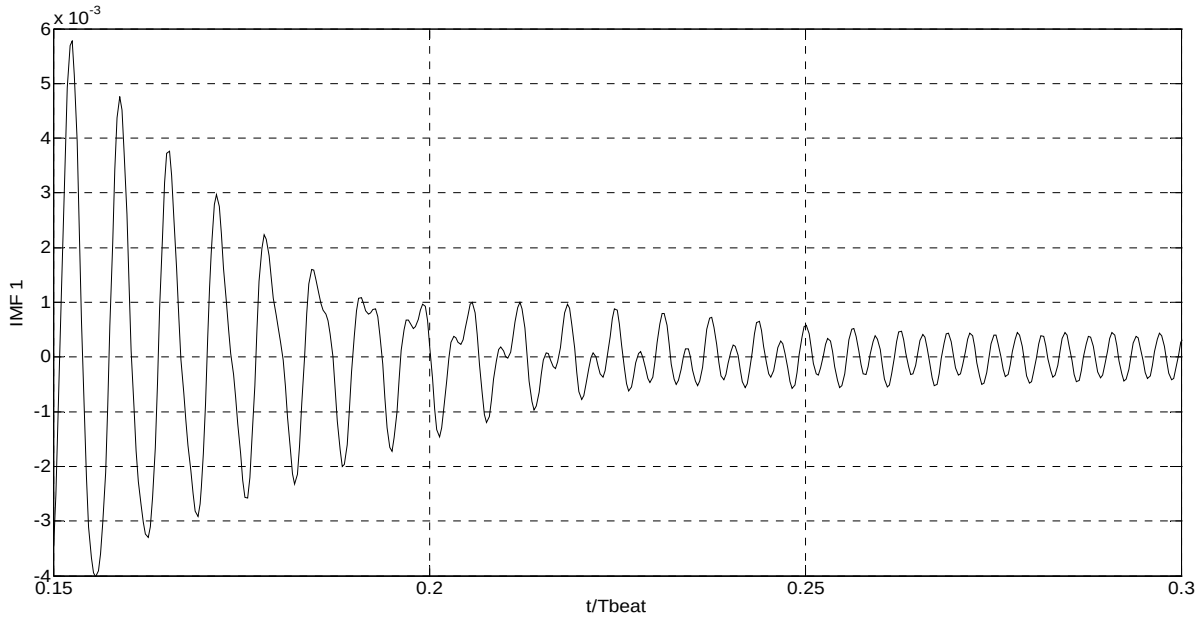

Figure 9: Close-up of the first IMF plotted versus the normalised time t/T_{beat}.

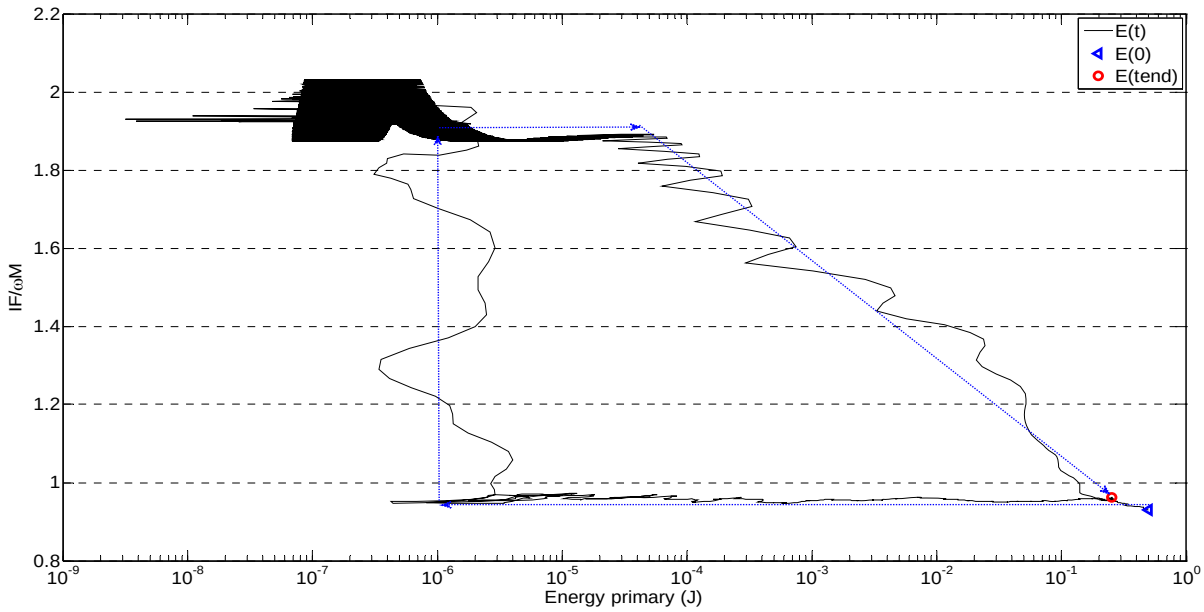

Figure 10: Frequency-energy related to the master plot of $E_N(IF(t))$, the IF is normalized with ω_M.

The IMF and the IF of the master response for $t>T_{beat}$ are plotted in Fig. 11. The figure highlights the existence of a mesoscale process where the time response of the master changes from a nearly periodic, where most of the energy is periodically transferred to and from the master with period T_{beat}, to a stationary state, where most of the energy is permanently stored into the satellite structure. During this *mesoscale* process two different alternating, or intermittent, phases are identified, corroborating the prediction made in section 3.1:

i. one governs the energy transfer to and from the master and is characterised by an IF roughly equal to ω_M;

ii. the other one is characterised by $\mathrm{IF} \approx 2\omega_M$, the primary and the most energetic resonators are energetically decoupled and the energy is reversibly exchanged between the master and a few resonators at high frequency.

iii. The time durations of these alternating phases change with time. Indicating with Δt_{ω_M} and $\Delta t_{2\omega_M}$ the nondimensional time durations, normalized with T_{beat}, at the beginning $\Delta t_{2\omega_M} \gg \Delta t_{\omega_M}$, as the time spends $\Delta t_{2\omega_M} \to 0$ and $\Delta t_{\omega_M} \to 1$.

iv. The mesoscale process duration T_{mes} is assumed to be the time when $\Delta t_{2\omega_M}$ becomes zero: for $t > T_{mes}$ no more intermittency is observed and the IF oscillates around the uncoupled frequency of the master.

It is worth to point out the sharp peaks in the IF plot observed after $\Delta t_{2\omega_M} = 0$, errors near the neighborhood of minimum amplitude locations, are consequence of violation of the Bedrosian theorem [15,16].

The points (i) to (iv) are strictly related to the time evolution of the envelope *A(t)*, previously discussed and highlighted in Fig. 7. It may be suspiring that for $t>T_{mes}$ no energy return is observed, even if the master remains in resonance with the most energetic resonators. The energy is reversibly exchanged, but its amplitude remains relatively small, close to the mean value $[E_N]$. An intuitive explanation for that can be found by considering the master velocity or energy expressions, eq.s (3, 5). For $t > 0$, the coherence among the modal components is progressively lost and each one contributes to the master energy with a fraction of its modal energy: a vast energy return is possible only if the initial coherence is regained. The numerical experiments have yielded two characteristic time scales: (i) for $t>T_{mes}$ the coherence among the modal components is regained roughly at each T_{beat} period, thus the master response has a clear almost periodic evolution, and (ii) for $t>T_{mes}$ the phases of the modal components are uncorrelated. It follows that the resultant force applied from the satellite has a small amplitude, even if the energy is almost completely stored into the CoAt, thus the motion of the master is roughly harmonic with frequency ω_M and small amplitude.

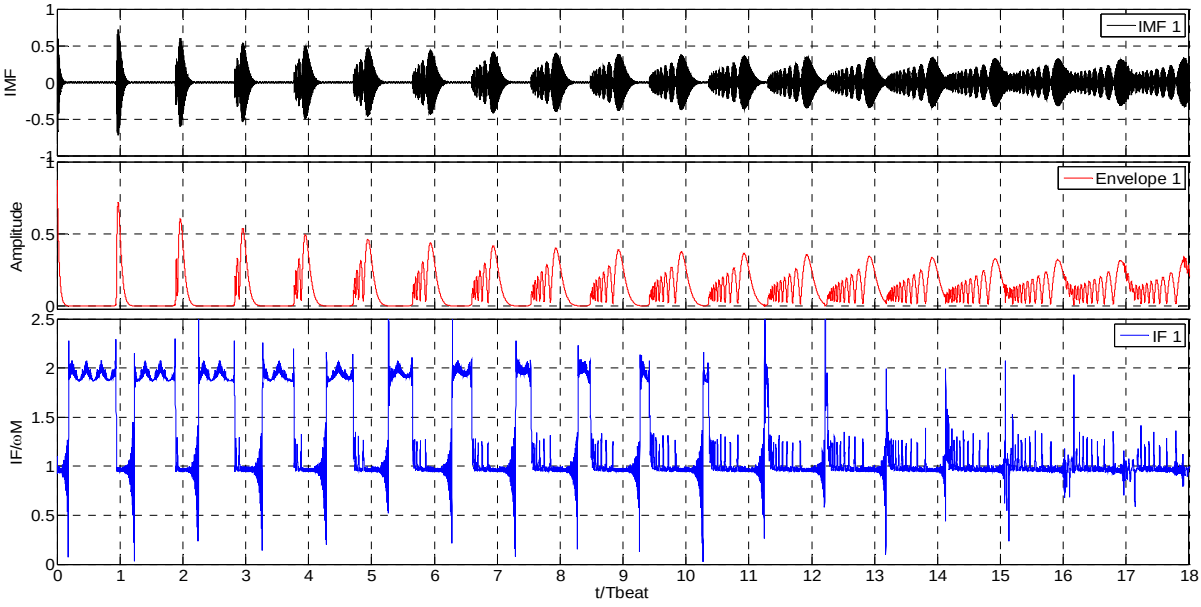

Figure 11: First IMF, instantaneous amplitude and frequency related to the master displacement.

Finally, it is indeed interesting to analyze the net force *F(t)* exerted from the satellite to the master. Eq. (1) is rearranged as follows:

$$\ddot{x}_N(t)+\left(\omega_M^2+\alpha\sum_{j=1}^{N-1}\omega_{0j}^2\right)x_N(t)=\alpha\sum_{j=1}^{N-1}\omega_{0j}^2 x_j(t)$$

where $\alpha = m/M$, thus:

$$F(t)=\alpha\sum_{j=1}^{N-1}\omega_{0j}^2 x_j(t)$$

The EMD is applied to *F(t)*: only one significant IMF is generated, the instantaneous amplitude and frequency are obtained with the NHT, and plotted in Fig. 12, respectively, for $t=[0,18T_{beat}]$. The time histories related to *F(t)* are qualitatively similar to the ones of $x_N(t)$, only the forward frequency jumps, from ω_M to $2\omega_M$, are slightly anticipated for *F(t)*, thus $x_N(t)$ remains longer and longer in resonance with *F(t)*, being the corresponding instantaneous amplitudes and frequencies strictly correlated. It arises one of the main advantages of using a LES instead of a conventional linear attachment or a NES: it allows keeping the amplitude of the force exchanged with the primary very small, even if most of the energy is efficiently targeted into the CoAt. For an efficient energy pumping neither strong nonlinear coupling nor a large mass for the attachment is needed.

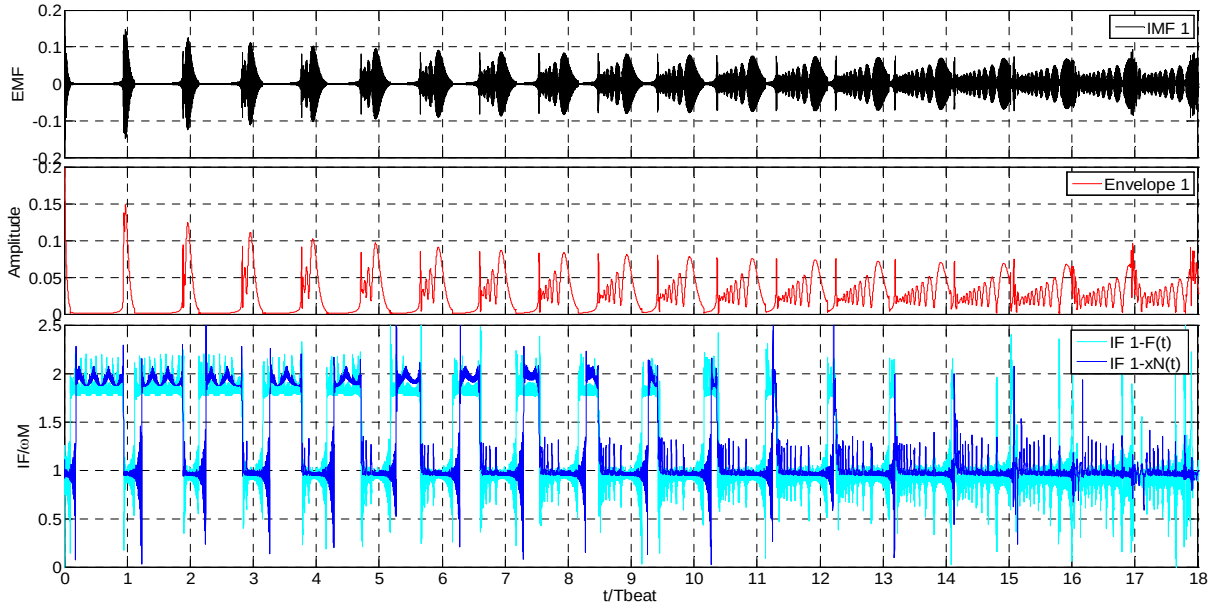

Figure 12: First IMF, instantaneous amplitude and frequency (in cyan) related to *F(t)*.

4 Concluding remarks

This paper reports the realization of an effective targeted energy pumping from a linear oscillator to a set of linear oscillators, coupled to it in parallel. The existence of a multiphase process where the instantaneous frequency, associated to the master response, is characterized by intermittency and assumes alternating values between ω_M and $2\omega_M$, has been unveiled. An intermittent frequency in a linear autonomous system is rather unexpected and, to the authors' knowledge, has never been reported before.

The results demonstrate the efficacy of using a CoAt as passive absorbers of broadband energy injected into the primary structure. Comparative studies have shown this special architecture allows trapping the energy more effectively than a nonlinear energy sink, or conventional linear absorbers. The proposed

device represents indeed a novelty in the field of energy pumping, up now focused on nonlinear attachments only.

The paper also explains the mechanism behind the apparent damping phenomenon, unveiling the existence of a mesoscale, where the master response changes from almost periodic, where most of the energy is periodically transferred to and from the master with a dominant period $T_{beat}=\pi N/\omega_M$, to a random noise motion, where the energy of the master remains very small, close to the mean value E_{tot}/N.

References

[1] H.J. Rice, J.R. McCraith, Practical non-linear vibration absorber design, Journal of Sound and Vibration 116 (3) (1987) 545–559.

[2] O. Gendelman, L.I. Manevitch, A.F. Vakakis, R.M. Closkey, Energy pumping in nonlinear mechanical oscillators:part I—dynamics of the underlying hamiltonian systems, Journal of Applied Mechanics 68 (2001) 34–41.

[3] A.F. Vakakis, O. Gendelman, Energy pumping in nonlinear mechanical oscillators: part II—resonance capture, Journal of Applied Mechanics 68 (2001) 42–48.

[4] A.F. Vakakis, Inducing passive nonlinear energy sinks in linear vibrating systems, Journal of Vibration and Acoustics 123 (3) (2001) 324–332.

[5] Y. S. Lee, G. Kerschen, A. F. Vakakis, P. Panagopoulos, L. A. Bergman, and D. M. Mc- Farland (2005), Complicated dynamics of a linear oscillator with an essentially nonlinear local attachment, Phys. D, 204, pp. 41–69.

[6] G. Kerschen, K. Worden, A. F. Vakakis, J.C Golinval (2006), Past, present and future of nonlinear system identification in structural dynamics, Mechanical Systems and Signal Processing, 20, 505–592 (2006).

[7] H. Bohr, “Almost Periodic Functions”. Chelsea, 1947.

[8] A. Giorgilli: “Notes on exponential stability of Hamiltonian systems”, in Dynamical Systems. Part I: Hamiltonian Systems and Celestial Mechanics, published by the Scuola Normale Superiore in Pisa.

[9] R.L. Weaver, “The effect of an undamped finite degree of freedom ‘fuzzy’ substructure: numerical solution and theoretical discussion”, Journal of Acoustical Society of America, vol.101, 3159-3164 (1996).

[10] R.S Langley, “Theoretical foundation of apparent damping and energy irreversible energy exchange in linear conservative dynamical systems”, Journal of Sound and Vibration, Vol. 206, pp. 624 - 626, 1997.

[11] A. Carcaterra, A. Akay, “Transient energy exchange between a primary structure and a set of oscillators: return time and apparent damping”, Journal of Acoustical Society of America, vol. 115, 683-696 (2004).

[12] A. Carcaterra, A. Akay, “Theoretical foundation of apparent damping and energy irreversible energy exchange in linear conservative dynamical systems”, Journal of Acoustical Society of America, 121, pp. 1971-1982, 2007.

[13] N. Roveri, A. Carcaterra, A. Akay, “Energy equipartition and frequency distribution in complex attachments”, *Journal of Acoustical Society of America*, vol. 126, 122-128 (2009).

[14] N. Roveri, A. Carcaterra, A. Akay, “Vibration absorption using non-dissipative complex attachments with impacts and parametric stiffness”, Journal of Acoustical Society of America, vol. 126, 2306-2314 (2009).

[15] S. Hahn, Hilbert transforms in signal processing. Artech House, 442 pp., 1995.

[16] N.E. Huang, Wu Z. Long S. R., Arnold K.C., Chen X., Blank K. (2009), On the instantaneous frequency, Advances in Adaptive Data Analysis, 1(2), 177-229 (2009).

View publication stats